

Investigation of Acoustic Waves generated by the Detonation Gun of a Zenith-M modernized Powerful Antihail Station

Gagik Ayvazyan

National Polytechnic University of Armenia, Armenia
agagarm@gmail.com (corresponding author)

Arman Vardanyan

National Polytechnic University of Armenia, Armenia | Barva Innovation Center, Armenia
vardanyan_arman@hotmail.com

Received: 22 August 2024 | Revised: 14 September 2024 | Accepted: 19 September 2024

Licensed under a CC-BY 4.0 license | Copyright (c) by the authors | DOI: <https://doi.org/10.48084/etasr.8800>

ABSTRACT

In this paper, a detonation gun of an antihail station was used to study acoustic waves as they propagated upward. The station's power was enhanced by placing a Hartmann resonance tube into the conical nozzle of the gun. Propagation speed, pressure-time waveform, and acoustic spectrum of the acoustic waves were determined. The propagation speed was approximately 890 m/s (Mach number ~2.6), and the initial (near-ground) intensity was 130-160 dB in the low-frequency range up to 200 Hz, where the energy distribution is relatively uniform. The results show that the antihail station can effectively influence atmospheric processes, either promoting rain precipitation or preventing hail formation.

Keywords-antihail station; detonation gun; acoustic waves; propagation characteristics

I. INTRODUCTION

Artificial influence on atmospheric processes is used to disperse fog, stimulate precipitation, prevent hail formation, improve air quality, and more. Currently, hygroscopic particles or special chemical solutions such as dry ice and silver iodide are widely used to affect the atmosphere [1]. However, this method requires the use of artillery, unmanned aerial vehicles, and aircrafts, which is very expensive. From an economic and environmental point of view, the most promising methods are those based on the impact on the atmosphere by acoustic waves [2, 3]. This approach involves no chemical pollution, no use of artillery or aircrafts, and the exposure process can be controlled remotely at a low cost. In scientific reports, the influence of acoustic waves on the atmosphere is primarily associated with the phenomenon known as acoustic agglomeration [4]. This refers to the collective effect of microparticles in an acoustic field. Droplets in clouds are influenced by forces that arise during the propagation of acoustic waves in the atmosphere, causing them to come closer and agglomerate [5, 6]. This enhances gravitational sedimentation, which in turn can help promote rain precipitation or prevent hail formation [3, 7, 8].

The study of acoustic waves and their effects on the atmosphere is primarily based on numerical simulation studies or experiments in a cloud chamber in a laboratory [5, 6, 9]. These studies have shown that the efficiency of acoustic agglomeration depends on the intensity, frequency, and time of

the acoustic action. Low-frequency and high-intensity acoustic waves are the most preferable. In particular, the simulation results have shown that the threshold Sound Pressure Level (SPL) for aerosol droplet agglomeration at 60 Hz is 89.4 dB [9]. This level is sufficient for noticeable vibrations of 10 μm droplets [5]. Simulation experiments in a cloud chamber have demonstrated that the threshold SPL ranges from 114 to 121 dB at frequencies of 35 to 100 Hz, and this level gradually increases with increasing frequency [6]. In situ meteorological monitoring results indicate that acoustic waves with a frequency of 20–250 Hz and near-ground intensities of up to 156 dB significantly impact the macro-characteristics of rainfall clouds, the microphysical structure of rain droplets and near-surface precipitation [3].

Previously, the Zenith acoustic antihail stations have been used to study acoustic waves generated from the Earth's surface into the atmosphere [8, 10]. These stations use detonation guns based on a Laval nozzle as a source of acoustic waves. The gun is a tube pinched in the middle, creating a carefully balanced asymmetrical hourglass shape. Its operation is based on the different properties of gases flowing at subsonic and supersonic speeds. The speed of the subsonic gas flow increases if the pipe carrying it narrows, due to the constant mass flow. In the "throat," where the cross-sectional area is minimal, the gas velocity locally becomes sonic. As the cross-sectional area of the nozzle increases, the gas begins to expand and the gas flow accelerates to supersonic speeds (Mach number > 1.0).

As a result of the burning of the gas mixture in the combustion chamber of the gun and the subsequent passage of gases through the Laval nozzle, a powerful acoustic wave or a series of waves is generated. These waves are directed upwards into the atmosphere to affect hail-bearing clouds. The results of our research showed that the acoustic waves generated by the antihail station exhibited a broadband frequency spectrum (up to 4 kHz) while their intensity did not exceed 100 dB [8, 10]. With such acoustic characteristics, it is impossible to conduct acoustic sounding of the fine structure of the troposphere at high altitudes (above 600 m) [10] and the effectiveness of the impact on hail-bearing clouds is very low. Based on this, we optimized the design of the station's detonation gun to increase its power.

This paper examines the propagation characteristics of acoustic waves generated by the redesigned detonation gun of the antihail station. The effectiveness of the station's impact on hail-bearing clouds is also discussed.

II. EXPERIMENTAL TECHNIQUE

For our ground-based experiments, we used the Zenith-M modernized powerful antihail station, installed at the experimental site of the Barva Innovation Center (Talin, Armenia). Figure 1 shows a photograph and the three-dimensional model construction of the detonation gun and antihail station.

The main component of the station is a detonation gun A, consisting of a combustion cylindrical combustion chamber (1) that has 1 m height and 0.53 m diameter, and an upward conic nozzle (2). The nozzle has an aperture angle of 8° , a height of 4 m, and an exit inner diameter of 0.8 m. The bottom of the combustion chamber is solidly mounted to a concrete pad by feet. At its base there are two air inlet ports (3), the gas injector (4), and the igniter (5). Propane-butane gaseous fuel from six bottles (6) passes through a reversible panel (7), which acts as a regulator. Manometers and safety valves control the gas pressure before it reaches the electromagnetic sluice gate that precedes the injector. All these automatic mechanisms are programmed through an electronic unit (8). A battery connected to a self-made silicon solar panel (9) provides the necessary power to operate the station [11]. A remote control activates the station, which can also be automatically powered on or off by a meteorological radar.

The amount of injected gas is selected to ensure the optimal composition of the mixture (4.6% propane and 3.6% butane), yielding the maximum explosion pressure. To ensure safety, gas sensors were used [12]. After igniting the gas-air mixture, the pressure in the combustion chamber increases, forming a shock wave and generating acoustic waves that are directed vertically upward into the atmosphere by the nozzle. Explosions occur in a pulse-periodic mode every 5 s. During one explosion, about 6–7 g of the mixture burns.

Increasing the power of a detonation gun can improve its effectiveness in influencing clouds. There are several ways to achieve this, including optimizing the design the design of the combustion chamber, refining the Laval nozzle, adjusting the operating parameters, and using more efficient and energy-intensive combustible mixtures [13]. In the Zenith-M antihail

station, we uniaxial placed a Hartmann Resonance Tube (HRT) (1) into the upward conical nozzle (2) to amplify acoustic waves (Figure 2).

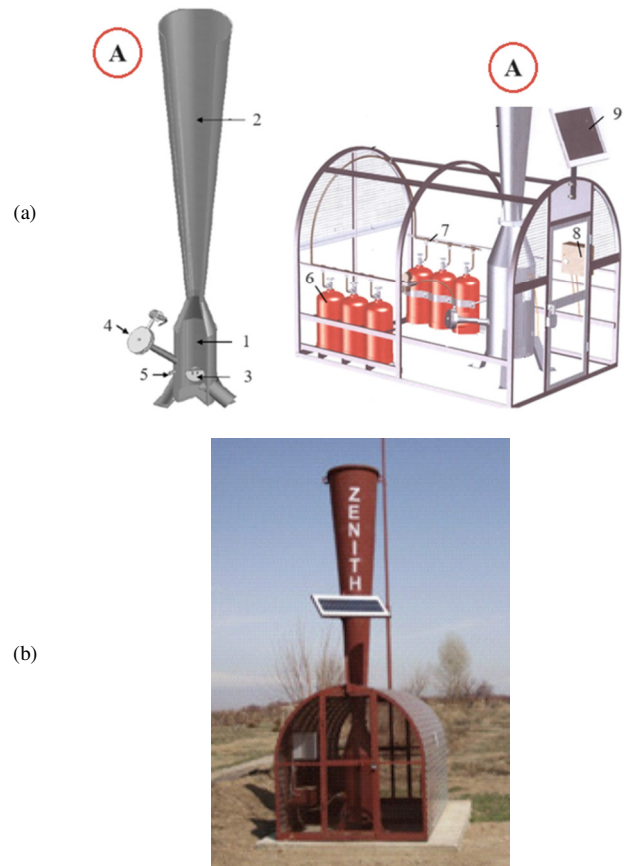


Fig. 1. (a) Three-dimensional construction and (b) photograph of the antihail station.

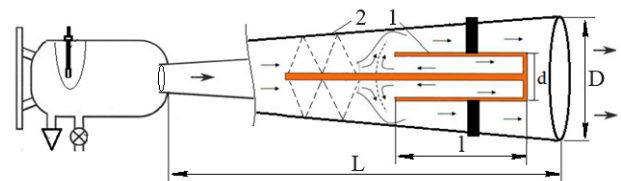


Fig. 2. Schematic diagram of detonation gun with Hartmann resonance tube.

The operation of the HRT is based on the well-known Hartmann–Sprengr effect, where gas-dynamic resonance occurs in a plugged vessel due to nonlinear self-oscillating gas pressure fluctuations arising from the supersonic gas flow around it [14]. This contributes to an increase in the intensity of the acoustic waves generated by the detonation tube. To select the optimal design and evaluate the geometric parameters of the HRT, we used the ANSYS Academic program. Theoretical estimates showed that the maximum amplification is provided by HRT diameter of $d=0.4-0.5D$ and a length of $l=0.3-0.45L$, where D and L are the diameter and length of the conic nozzle, respectively. It should be noted the authors in [15] have

successfully used aerodynamic Hartmann type generators in acoustic air cleaning equipment for the acoustic agglomeration of particles.

Acoustic characteristics were measured using two dynamic pressure sensors (PCB 113B26) and highly sensitive sound meters (Bruel & Kjaer). One measuring device was positioned near the muzzle, while the second was placed at a height of 25 m above it. Electrical signals were simultaneously recorded by a computer and analyzed using a specialized program for performing frequency analysis using Fast Fourier Transform (FFT).

III. RESULTS AND DISCUSSION

Figure 3 shows typical pressure-time waveforms at different measuring points. It can be seen that the first pulses have a short duration, after which acoustic oscillations with wider and damping pulses are observed. This pressure-time signature is typical for a wide range of shock-acoustic wave sources, including firearms of all scales. In studies, these signals are characterized as Friedlander pulses [16].

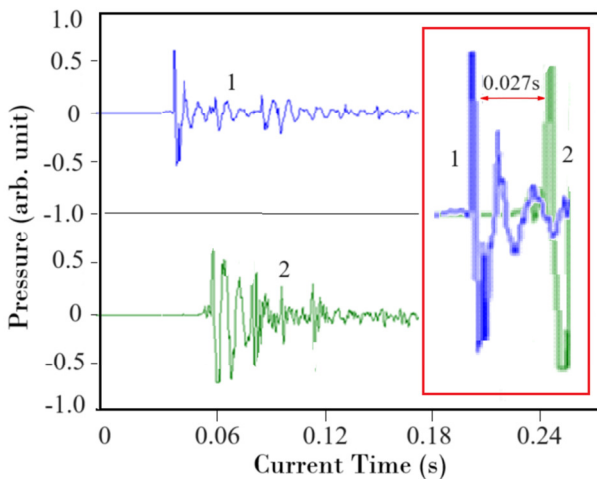


Fig. 3. Waveforms at different measuring points: near the muzzle (1) and at a height of 25 m (2).

The total duration of the signals does not exceed 0.2 s (Figure 3). The time interval between the leading edges of the first pulses at both measuring points is about 0.027 s, therefore, the calculated propagation speed of the acoustic waves is approximately 890 m/s (Mach number ~2.6). This means that in 2.0-2.5 s, acoustic waves can reach heights characteristic of hail-bearing clouds (1.5–2.0 km in the case of Armenia).

Figure 4 shows the logarithmic acoustic spectrum at both measurement points obtained by applying FFT to the corresponding waveforms. The acoustic waves generated by the detonation gun have a broadband frequency spectrum. Significant energy was observed in the low-frequency range up to 200 Hz, where the energy distribution is relatively uniform. Noticeable high-frequency components also contribute to the overall acoustic signature. The intensity of the acoustic waves decreases with increasing frequency. The attenuation in the

frequency range of 10–104 Hz is approximately -120 dB, with the attenuation rate increasing when the frequency exceeds 900 Hz. Some differences in the waveforms (Figure 3) and frequency spectra (Figure 4) of the acoustic waves at both measurement points are likely due to the absorption and scattering of the waves during propagation. The studied antihail station with an HRT into the conical nozzle provides higher intensities of the detonation acoustic waves (130-160 dB in the low-frequency range) compared to the station without the HRT [8]. This is mainly due to the interaction of the shock wave and the resonance oscillations that occur in-side the detonation gun.

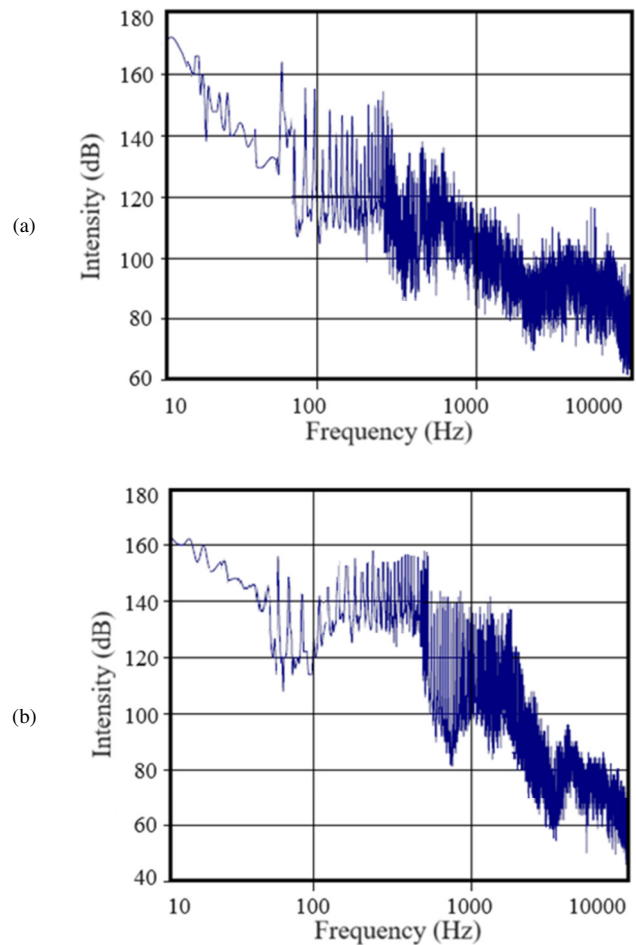


Fig. 4. Logarithmic acoustic spectrum at different measuring points: near the muzzle (a) and at a height of 25 m (b).

Here we analyze the effectiveness of the Zenith-M powerful antihail station to influence atmospheric processes. The impact of acoustic waves on cloud droplets is characterized by the relative displacement of the droplets according to [17]:

$$K = \frac{A_r}{A} = \left[1 + \left(\frac{A_p r^2 f}{9\gamma} \right)^2 \right]^{-1/2} \tag{1}$$

where A is the amplitude of the acoustic wave, A_r is the vibration amplitude of the droplet, r is the radius of the droplet,

ρ is the density of the droplet, γ is the dynamic viscosity of the medium, and f is the frequency of the acoustic wave.

Figure 5 shows the calculated curves of the relative displacement of droplets depending on their radius at different frequencies of acoustic waves. Calculations were carried out for typical values of the radius of droplets in natural clouds, namely $r = 0.5\text{--}20\ \mu\text{m}$.

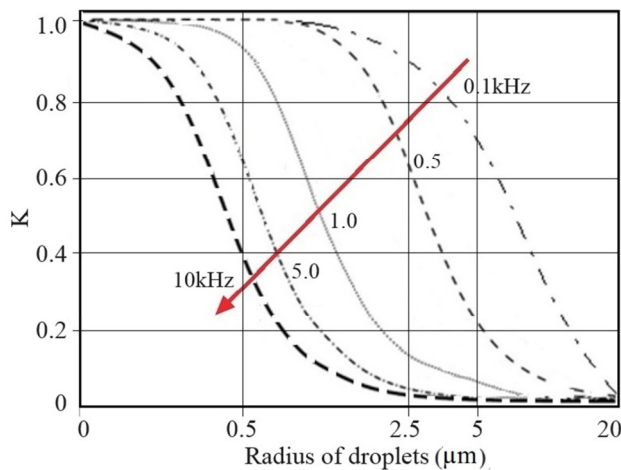


Fig. 5. Relative displacement of droplets (K) depending on their radius at different frequencies of acoustic waves.

From the presented dependencies in Figure 5, it follows that for maximum displacement of droplets, it is necessary to use low-frequency acoustic waves. Reducing the droplet size leads to an increase in the relative displacement of droplets, especially at high frequencies. The dependence of droplet displacement on their size is insignificant for low-frequency acoustic waves. Thus, low-frequency acoustic waves are the most preferable from the point of view of active influence on the atmosphere. The Zenith-M antihail station generates low-frequency waves with significant energy. Additionally, the initial (near-ground) intensity of acoustic waves in the low-frequency range is approximately 160 dB, which is sufficient to significantly influence the macro-characteristics of clouds [3]. Using the inverse square law taking into account sound attenuation in the atmosphere, it is possible to estimate the intensity of acoustic waves in the acoustic agglomeration zone at altitudes of 1.5–2.0 km. The calculated values are 93–97 dB, which exceeds the theoretical threshold level for effective agglomeration of aerosol droplets [9]. On the other hand, these values are almost 20 dB lower than the results of simulation experiments in a cloud chamber [6], but the experiments did not take into account the trigger and periodic effects of acoustic waves on the cloud. According to [2], these effects are key positive factors of acoustic atmospheric impact. It should be noted that the Zenith-M antihail station provides up to 12 explosions per minute, and the total number of shots in one package is 120.

IV. CONCLUSION

To influence atmospheric processes, particularly to promote rain or prevent hail formation, acoustic waves are generated

from the Earth's surface using a detonation gun based on a Laval nozzle. Increasing the power of the detonation gun can improve its efficiency in affecting clouds. This paper studies the propagation characteristics of acoustic waves generated by a redesigned detonation gun of an antihail station. It is shown that installing a Hartmann resonance tube in the upward conical nozzle increases the power of the detonation gun due to additional resonant oscillations. The propagation speed of acoustic waves was approximately 890 m/s, and the initial intensity was 130–160 dB in the low-frequency range, up to 200 Hz, which is more than 30% higher than the performance of a gun without a Hartmann tube. A powerful anti-hail station provides acoustic waves for effective impact on hail-bearing clouds. It should be noted that the studies were conducted in the peak direction of wave propagation. Similar investigations at different angles, including the horizontal direction (on the Earth's surface), are of particular interest. This is important for determining the area of active influence on the cloud and from the point of view of environmental safety. These issues will be our focus in further research.

ACKNOWLEDGMENT

This work was supported by the Science Committee of the Republic of Armenia (research projects no. 21AG-2B011 and 21T-2D023).

REFERENCES

- [1] M. H. Kim, J. Lee, and S.-J. Lee, "Hail: Mechanisms, monitoring, forecasting, damages, financial compensation systems, and prevention," *Atmosphere*, vol. 14, no. 11, pp. 1642–4654, Oct. 2023, <https://doi.org/10.3390/atmos14111642>.
- [2] J. Wei, J. Qiu, T. Li, Y. Huang, Z. Qiao, J. Cao, D. Zhong, and G. Wang, "Cloud and precipitation interference by strong low-frequency sound wave," *Science China Technological Sciences*, vol. 64, no. 2, pp. 261–272, Apr. 2021, <https://doi.org/10.1007/s11431-019-1564-9>.
- [3] Y. Shi, Z. Qiao, G. Wang, and J. Wei, "In situ experimental study of cloud-precipitation interference by low-frequency acoustic waves," *Remote Sensing*, vol. 15, no. 4, pp. 993–1004, Feb. 2023, <https://doi.org/10.3390/rs15040993>.
- [4] Z. Zhang, Z. Deng, P. Luo, G. Shen, and S. Zhang, "Review of acoustic agglomerations technology research," *ACS Omega*, vol. 9, no. 20, pp. 21690–21705, May 2024, <https://doi.org/10.1021/acsomega.3c08815>.
- [5] F.-F. Li, Y.-H. Jia, G.-Q. Wang, and J. Qiu, "Mechanism of cloud droplet motion under sound wave actions," *Journal of Atmospheric and Oceanic Technology*, vol. 37, no. 9, pp. 1539–1550, July 2020, <https://doi.org/10.1175/JTECH-D-19-0210.1>.
- [6] J. Qiu, L.-J. Tang, L. Cheng, G.-Q. Wang, and F.-F. Li, "Interaction between strong sound waves and cloud droplets: Cloud chamber experiment," *Applied Acoustics*, vol. 176, no. 4, May 2021, Art. no. 107891, <https://doi.org/10.1016/j.apacoust.2020.107891>.
- [7] V. M. Rodríguez-Moreno and J. Estrada-Ávalos, "Heavy rainfall events in selected geographic regions of Mexico, associated with hail cannons," *Forecasting*, vol. 6, no. 2, pp. 418–433, June 2024, <https://doi.org/10.3390/forecast6020023>.
- [8] A. R. Aramyan, G. R. Aramyan, K. P. Haroyan, G. A. Galechyan, A. A. Vardanyan, G. A. Danielyan, H. B. Nersisyan, and S. Bilen, "A study of acoustic waves generated by the shock wave of an antihail gun," *Acoustical Physics*, vol. 57, no. 3, pp. 432–436, May 2011, <https://doi.org/10.1134/S1063771011030031>.
- [9] F. Li, H. Cao, Y. Jia, Y. Guo, and J. Qiu, "Interaction between strong sound waves and aerosol droplets: Numerical simulation," *Water*, vol. 14, no. 10, pp. 1661–1680, May 2022, <https://doi.org/10.3390/w14101661>.

- [10] I. Chunchuzov, S. Kulichkov, O. Popov, V. Perepelkin, A. Vardanyan, and G. Ayvazyan, "Atmospheric boundary layer as a laboratory for modeling infrasound propagation and scattering in the atmosphere," *Pure and Applied Geophysics*, vol. 178, no. 2, pp. 2611–2625, July 2021, <https://doi.org/10.1007/s00024-020-02507-y>.
- [11] G. Y. Ayvazyan, R. N. Barseghyan, and S. A. Minasyan, "Optimization of surface reflectance for silicon solar cells," *Green Energy and Smart Grids. E3S Web of Conferences*, vol. 69, pp. 1–4, Nov. 2018, Art. no. 01008, <https://doi.org/10.1051/e3sconf/20186901008>.
- [12] G. Ayvazyan, K. Ayvazyan, L. Hakhoyan, and A. Semchenko, "NO₂ gas sensor based on pristine black silicon formed by reactive ion etching," *Physica Status Solidi RRL*, vol. 17, no. 9, Mar. 2023, Art. no. 2311158, <https://doi.org/10.1002/pssr.202300058>.
- [13] M. W. Khalid and M. Ahsan, "Computational fluid dynamics analysis of compressible flow through a converging-diverging nozzle using the k-ε turbulence model," *Engineering, Technology & Applied Science Research*, vol. 10, no. 1, pp. 5180–5185, Feb. 2020, <https://doi.org/10.48084/etasr.3140>.
- [14] A. Belousov, V. Lushpeev, A. Sokolov, R. Sultanbekov, Y. Tyan, E. Ovchinnikov, A. Shvets, V. Bushuev and S. Islamov, "Hartmann–Sprenger energy separation effect for the quasi-isothermal pressure reduction of natural gas: Feasibility analysis and numerical simulation," *Energies*, vol. 17, no. 9, pp. 2010–2035, Apr. 2024, <https://doi.org/10.3390/en17092010>.
- [15] V. Vekteris, D. Ozarovskis, I. Moksins, V. Turla, and E. Jurkonis, "An efficiency study of the aerodynamic sound generators suitable for acoustic particle agglomeration," *Engineering, Technology & Applied Science Research*, vol. 10, no. 2, pp. 5561–5564, Apr. 2020, <https://doi.org/10.48084/etasr.3426>.
- [16] R. S. Birch, S. N. Gerges, and E. F. Vergara, "Design of a pulse generator and shock tube for measuring hearing protector attenuation of high-amplitude impulsive noise," *Applied Acoustics*, vol. 64, no. 3, pp. 269–286, Mar. 2003, [https://doi.org/10.1016/S0003-682X\(02\)00088-9](https://doi.org/10.1016/S0003-682X(02)00088-9).
- [17] V. Vekteris, I. Tetsman, and V. Moksins, "Experimental investigation of influence of acoustic wave on vapour precipitation process," *Engineering, Technology & Applied Science Research*, vol. 3, no. 2, pp. 408–412, Apr. 2013, <https://doi.org/10.48084/etasr.303>.